Spinon heat transport and spin-phonon interaction in the antiferromagnetic spin-1/2 Heisenberg chain cuprates Sr_2CuO_3 and $SrCuO_2$

N. Hlubek,[1] X. Zotos,[2,3] S. Singh,[1,4,5] R. Saint-Martin,[4] A. Revcolevschi,[4] B. Büchner,[1] and C. Hess[1]

[1] *IFW-Dresden, Institute for Solid State Research, P.O. Box 270116, D-01171 Dresden, Germany*
[2] *Department of Physics and Institute of Theoretical and Computational Physics, University of Crete, Greece*
[3] *Foundation for Research and Technology-Hellas, PO Box 2208, 71003 Heraklion, Greece*
[4] *Laboratoire de Physico-Chimie de L'Etat Solide, ICMMO, UMR8182, Université Paris-Sud, 91405 Orsay, France*
[5] *Indian Institute of Science Education and Research, 900 NCL Innovation Park, Pashan, Pune 411008, India*

(Dated: February 20, 2012)

We have investigated the thermal conductivity $\kappa_{\rm mag}$ of high-purity single crystals of the spin chain compound Sr_2CuO_3 which is considered an excellent realization of the one-dimensional spin-1/2 antiferromagnetic Heisenberg model. We find that the spinon heat conductivity $\kappa_{\rm mag}$ is strongly enhanced as compared to previous results obtained on samples with lower chemical purity. The analysis of $\kappa_{\rm mag}$ allows to compute the spinon mean free path $l_{\rm mag}$ as a function of temperature. At low-temperature we find $l_{\rm mag} \sim 0.5\,\mu$m, corresponding to more than 1200 chain unit cells. Upon increasing the temperature, the mean free path decreases strongly and approaches an exponential decay $\sim \frac{1}{T} \exp T_u^*/T$ which is characteristic for umklapp processes with the energy scale $k_B T_u^*$. Based on Matthiesen's rule we decompose $l_{\rm mag}$ into a temperature-independent spinon-defect scattering length l_0 and a temperature dependent spinon-phonon scattering length $l_{\rm sp}(T)$. By comparing $l_{\rm mag}(T)$ of Sr_2CuO_3 with that of $SrCuO_2$, we show that the spin-phonon interaction, as expressed by $l_{\rm sp}$ is practically the same in both systems. The comparison of the empirically derived $l_{\rm sp}$ with model calculations for the spin-phonon interaction of the one-dimensional spin-1/2 XY model yields reasonable agreement with the experimental data.

PACS numbers: 75.40.Gb, 66.70.-f, 68.65.-k, 75.10.Pq

I. INTRODUCTION

The physics of low-dimensional quantum magnets has recently attracted considerable attention by experimentally and theoretically working scientists because intriguing properties are found. Such systems exhibit a variety of unusual ground states and exotic elementary excitations which, in some cases are well accessible by theoretical treatments. An important class of materials which host such quantum magnets is formed by copper-oxides (cuprates) which feature Cu^{2+}-ions which, through their $3d^9$ configuration, generate $S = 1/2$ sites. The type and strength of the interaction between these spins depends crucially on the structure of the material. For example, amongst the cuprates there are model systems which realize $S = 1/2$ arrangements with strong antiferromagnetic (AFM) Heisenberg-type interaction ($J/k_B \sim 2000\,$K) in the form of square lattices, two-leg spin ladders and chains.[1–5] About 10 years ago it was discovered, that in all these different systems their magnetic excitations give rise to a highly anisotropic thermal conductivity tensor of the respective materials, with an unexpectedly large magnetic contribution along the directions of large AFM exchange. This finding opened up a new route to investigating the generation, scattering and dissipation of magnetic quasiparticles (complementary to neutron scattering and magnetic resonance experiments) through analyzing the magnetic thermal conductivity $\kappa_{\rm mag}$.[6–16] Among these findings, the results for compounds which realize the one-dimensional $S = 1/2$ AFM Heisenberg model (1D-AFM-HM) are particularly interesting because fundamental conservation laws predict ballistic heat transport in these systems.[17,18] This means that in the 1D-AFM-HM model, an *infinite* magnetic heat conductivity is expected. Despite this rigorous prediction, in any real system, the transport is dissipative, due to extrinsic scattering mechanisms. Nevertheless, an unprecedentedly large $\kappa_{\rm mag}$ has been observed in ultra-pure samples of the zig-zag chain compound $SrCuO_2$.[15,19] More specifically, upon enhancing the chemical purity of the compound, $\kappa_{\rm mag}$ becomes i) increasingly larger, and ii) even for the highest purity level it can be fully described (in the framework of a simple kinetic model) by considering spinons scattering off impurities and phonons only, where the impurity scattering fully accounts for purity dependence of $\kappa_{\rm mag}$ and the phonon scattering prevails at elevated temperatures. This is indeed consistent with the predicted ballistic transport since no further scattering (i.e. spinon spinon scattering) mechanism needs to be invoked.[15] Furthermore, the analysis of the data yields very clean data for the spinon-phonon scattering, for which a full theoretical description is still lacking.

In the zig-zag chain compound $SrCuO_2$, two $S = 1/2$ chains with large AFM exchange are tied together by a significant but frustrated intrachain exchange. In this paper we extend the previous findings for $SrCuO_2$ to the *single*-chain material Sr_2CuO_3, where such complications are absent. We find that in high purity samples of this

compound $\kappa_{\rm mag}$ is strongly enhanced as compared to previous results[8,20] for lower purity. Upon comparing the dependence of $\kappa_{\rm mag}$ on the nominal purity level we observe that $\kappa_{\rm mag}$ of Sr_2CuO_3 depends in a similar fashion on the purity of the material like $SrCuO_2$. More specifically, within a simple kinetic model[8] the spinon mean free path $l_{\rm mag}$ can be decomposed into terms which describe spinon-defect and spinon-phonon scattering as is the case for the zig-zag chain compound. We show that using an empirical formula[8] for describing the spinon-phonon scattering that the strength of this mechanism is practically indistinguishable for both materials. Going beyond this empirical approach we model the spinon-phonon scattering by employing results for the spin-phonon interaction of the XY-model which further underpins these findings.

II. MATERIALS DETAILS

The main building blocks of Sr_2CuO_3 are corner sharing chains formed by CuO_3 plaquettes.[21] The chains are parallel to the crystallographic b-axis in Sr_2CuO_3. The intrachain exchange interaction between neighboring Cu^{2+} sites is mediated by 180° superexchange through the oxygen and with $J/k_B \approx 2150 - 3000\,\mathrm{K}$[5,22,23] is among the largest among known Heisenberg spin chain materials. The Cu-O-Cu chains are separated by Sr atoms, leading to an extremely small interchain interaction of $J_{\rm perp}/k_B \approx 0.02\,\mathrm{K}$. Furthermore, muon spin rotation and neutron scattering measurements[24,25] show that this material orders three-dimensionally only below the Néel temperature of $T_N \approx 5.4\,\mathrm{K}$. These properties make Sr_2CuO_3 an excellent realization of a $S = 1/2$ Heisenberg chain for temperatures $T > 5.4\,\mathrm{K}$. While Sr_2CuO_3 consists of isolated chains, the main structural element in $SrCuO_2$ is formed by CuO_2 zig-zag ribbons, which run along the crystallographic c-axis. Each ribbon can be viewed as made of two parallel chains of corner-sharing CuO_2 plaquettes, where the straight Cu-O-Cu bonds between corner-sharing plaquettes of each double-chain structure result in a very large antiferromagnetic intrachain exchange coupling $J/k_B \approx 2100 - 2600$ K of the $S = 1/2$ spins at the Cu^{2+}sites.[5,26] The interchain coupling J' between Cu^{2+}-sites of two edge-sharing plaquettes is much weaker ($\left|J'\right|/J \approx 0.1 - 0.2$).[5,27] Frustration of this exchange interaction and presumably quantum fluctuations prevent three-dimensional long range magnetic order of the system at $T > T_N \approx 1.5 - 2\,\mathrm{K} \approx 10^{-3} J/k_B$ K.[28,29] Hence, at significantly higher T the two chains within one double chain structure are usually regarded as magnetically independent. In fact, low-T (12 K) inelastic neutron scattering spectra of the magnetic excitations can be very well described within the $S = 1/2$ Heisenberg antiferromagnetic chain model.[26]

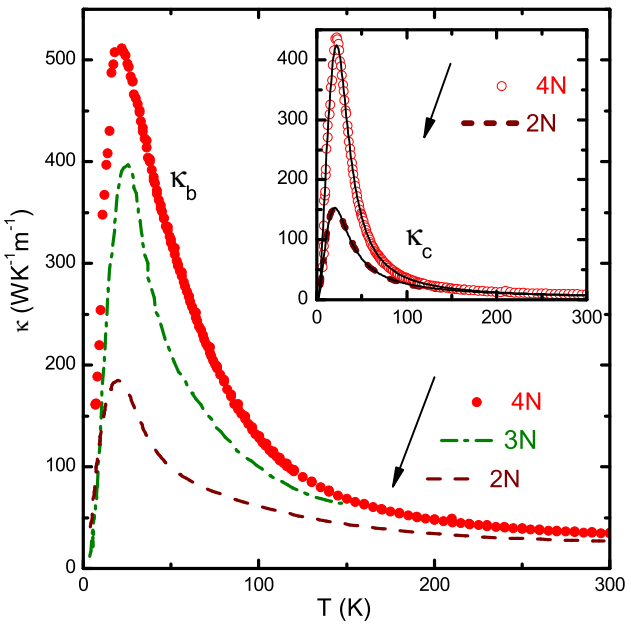

Figure 1: Thermal conductivity of Sr_2CuO_3 parallel to the spin chains along κ_b for various purities. The dashed lines represent results from Sologubenko et. al. with 2N purity, reproduced from Ref. 7. The dash-dotted line has been obtained by Kawamata et. al. for 3N purity and is reproduced from Ref. 20. Inset: Thermal conductivity of Sr_2CuO_3 perpendicular to the spin chains along κ_c for 2N (also reproduced from Ref. 7) and 4N purity. The solid lines are fits to the Callaway model.

III. EXPERIMENTAL DETAILS

Large single crystals of pure Sr_2CuO_3 were grown by the traveling solvent floating zone method.[30] The feed rods were prepared using the primary chemicals CuO and $SrCO_3$ with 4N (99.99%) purity. The crystals react rather rapidly with water. A hydroxide layer is formed at the surface of the crystals, after a short exposure to air.[31,32] Therefore the crystals were annealed at 900°C in an oxygen atmosphere for three days before further treatment. This reverts the hydroxide layer back to Sr_2CuO_3, although in a polycrystalline form.

The crystallinity and stoichiometry of all crystals were checked under polarized light and by energy-dispersive X-ray spectroscopy, respectively. For the transport measurements rectangular samples with typical dimensions of $(2 \cdot 0.5 \cdot 0.5)$ mm^3 were cut from the crystals for each doping level with an abrasive slurry wire saw. Four-probe measurements of the thermal conductivity κ were performed[33] in the 7–300 K range with the thermal current along the b and c-axes (κ_b and κ_c respectively).

IV. EXPERIMENTAL RESULTS

Fig. 1 presents our findings for the heat conductivity of Sr_2CuO_3, measured with the heat current parallel to the b and c axes, i.e. parallel and perpendicular to the chains in the material. We focus first on the temperature dependence of the thermal conductivity perpendicular to the spin chain, κ_c, which is shown in the inset of the figure. Along this direction, the heat conductivity of this electrically insulating material is purely phononic: As a function of temperature, it shows a characteristic peak at $T = 22\,\mathrm{K}$, and then strongly decreases upon further rising the temperature. The height of the peak sensitively depends on the density of impurities in the system, which generate phonon-defect scattering. This can be well inferred by comparing our data for a 4N-purity material with that of 2N (i.e., 99%) purity, taken from Ref. 8. For this lower-purity sample the overall magnitude of κ_c is strongly reduced as is expected for typical phonon heat conductors.[34] In fact, the data for both purities can be well described in the framework of a model by Callaway[35], where the difference between both curves is largely captured by different point defect scattering strength (see Appendix).

The thermal conductivity parallel to the chain, κ_b, is shown in the main panel of Fig. 1. κ_b exhibts a peak at the same position as observed for κ_c. However, the peak is much broader and the overall magnitude of κ_b is significantly larger than that of the purely phononic κ_c, which is the signature of a substantial magnetic contribution in this material, i.e., the heat current parallel to the spin chain is carried not only by phonons but also by spinons.[8] For our 4N purity sample, the anisotropy between κ_b and κ_c is roughly constant above 100 K and approximately $\kappa_b/\kappa_c \approx 3.5$. This is significantly larger than the previously reported[8] anisotropy for 2N-purity Sr_2CuO_3 and provides clear evidence that the enhanced purity leads to a relative enhancement of the spinon contribution to the overall heat conductivity. The purity dependence of κ_b can directly be read off from the figure where we compare our findings with experimental data for 3N (99.9% purity) and 2N purity samples of Sr_2CuO_3, reproduced from Ref. 20 and Ref. 8, respectively. From low to intermediate temperatures [7 K – 150 K], the heat conductivity is strongly enhanced upon increasing the sample purity. At higher temperatures this purity dependence becomes weaker since the curves approach each other. Apparently it is possible to separate the thermal conductivity into two distinct regimes, where different scattering processes dominate. At low-T, the extreme sensitivity to impurities suggests, that spinon scattering off defects is dominating. At high-T, a further extrinsic scattering mechanism – spinon-phonon scattering[8] – becomes dominating as a consequence of increasing phonon population, which leads to the very similar $\kappa_{b,2N}$ and $\kappa_{b,4N}$ for $T \gtrsim 200\,\mathrm{K}$.

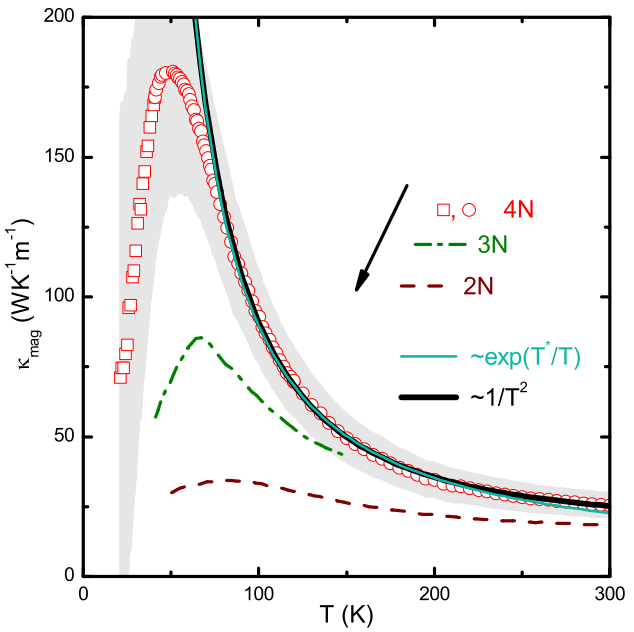

Figure 2: Estimated magnetic thermal conductivity of Sr_2CuO_3 for 4N (circles, squares), 3N (dash-dotted line)[20], and 2N (dashed line)[7] purity. The shaded area illustrates the uncertainty from the estimation of the phononic background. The 4N results shown in squares instead of circles have a large uncertainty. The thick solid line is a fit for $T > 80\,\mathrm{K}$ with $\kappa_{\mathrm{mag,fit1}} \sim 1/T^2$. The thin solid line is a fit with $\kappa_{\mathrm{mag,fit2}} \sim \exp(T^*/T)$.

V. DATA ANALYSIS AND DISCUSSION

A. The spinon heat conductivity of Sr_2CuO_3

The thermal conductivity parallel to the chain is composed of a magnetic and phononic contribution $\kappa_b = \kappa_{\mathrm{mag}} + \kappa_{b,\mathrm{ph}}$. In order to extract the heat conductivity of the spin chain the phononic background is approximated as $\kappa_{b,\mathrm{ph}} \approx \kappa_c$. This simple assumption is reasonable, since the purely phononic anisotropy between κ_a and κ_c is small.[7,8] Therefore $\kappa_{b,\mathrm{ph}}$ is not expected to be much different. The thus obtained spinon heat conductivity $\kappa_{\mathrm{mag}} = \kappa_b - \kappa_c$ for the 4N sample, as well as the results from literature for 3N and 2N, for which κ_{mag} was extracted in a similar way,[7,8,20] are shown in Fig. 2. Below $T \lesssim 40\,\mathrm{K}$, i.e., in the vicinity of the peak of $\kappa_{\mathrm{ph},b}$, errors become large and the data in this range are neglected for further analysis. For higher T, the possible uncertainty of κ_{mag} is around ±15%, which accounts for the individual errors of κ_b and κ_c.

Starting from low-T, κ_{mag} of the 4N sample increases almost linearly towards a peak. The uncertainty is quite large in the temperature regime, and hence an increase with a higher power[36,37] of T in this regime ($T < 40$ K) cannot be excluded. However, in the simplest case of a temperature independent spinon-defect

scattering rate, one expects $\kappa_{\rm mag}$ to be directly proportional to the thermal Drude weight $D_{\rm th}$, which also increases linearly with temperature at low-T up to $T \sim 0.15J/k_B \sim 300$ K.[14,38–41] The peak is quite pronounced and found at ∼48 K with a maximum value of about 180 $\mathrm{Wm^{-1}K^{-1}}$. The peak is followed by a strong decrease for higher T. Such a temperature dependence can not be accounted for from the T-dependence of the thermal Drude weight, since it is expected to decrease only at very high $T \gtrsim 0.6J/k_B \sim 1200$ K.[38–41] Instead, the decrease is consistent with our earlier notion of dominant spinon-phonon scattering at high-T. $\kappa_{\rm mag}$ of the 3N and 2N samples is qualitatively very similar to that of the 4N sample but is increasingly suppressed with growing impurity level, accompanied with a shift of the peak-position of $\kappa_{\rm mag}$ towards higher temperatures. Furthermore, the curves approach each other with increasing temperature, as the κ_b data.

Chernyshev and Rozhkov have proposed a model which describes $\kappa_{\rm mag}$ of Sr_2CuO_3 at the 2N purity level very well.[36,37] However, a similarly convincing description of our data for the 4N sample is not possible. The same holds for the double chain material $SrCuO_2$. Spin-phonon drag has been suggested as a possible explanation for the failure of the model.[42] Recently there has been substantial progress in the formal theoretical treatment of this phenomenon.[43] However, specific model calculations have not yet been performed for the materials under scrutiny here. It thus remains unclear whether spin-phonon drag plays a significant role in our experimental data, and we analyse $\kappa_{\rm mag}$ without taking into account a possible contribution due to this effect.

The temperature dependence of $\kappa_{\rm mag}$ at high temperature $T \gtrsim 80$ K up to room temperature can equally well be described by either $\kappa_{\rm mag} \propto 1/T^2 + \text{const.}$ or $\kappa_{\rm mag} \propto \exp(T_u^*/T)$, with T_u^* a characteristic energy scale. Fig. 2 shows the corresponding fits. While the physical meaning of the former functional form remains elusive, one expects the exponential one for spinons scattering off phonons from general considerations for Umklapp processes.[44]

B. The spinon mean free path

We proceed by calculating the mean free path of the spinons, $l_{\rm mag}$, from the experimental $\kappa_{\rm mag}$ by[7,8,14,15,45]

$$l_{\rm mag} = \frac{3\hbar}{\pi N_s k_B^2 T}\kappa_{\rm mag}, \qquad (1)$$

where N_s is the number of spin chains per unit area. The thus extracted mean free paths are shown in Fig. 3. $l_{\rm mag}(T)$ is very large at low temperature (∼ 0.5 µm) and decreases strongly with increasing temperature, consistent with the above already inferred increasing importance of spinon-phonon scattering. While the high temperature data ($T \gtrsim 100$ K) reflects well the exponential suppression of $\kappa_{\rm mag}$, i.e. $l_{\rm mag} \sim \frac{1}{T}\exp T_u^*/T$, (shown as a dotted line in Fig. 3), the low temperature data clearly deviate from this functional form, which indicates that spinon-defect scattering becomes important. In order to test this notion, we compare in Fig. 3 these $l_{\rm mag}$ data for the 4N sample with fits to the results of 2N and 3N purity samples as given in Refs. 8,20. As expected, the enhanced impurity density in these samples causes a corresponding reduction of $l_{\rm mag}$ at low temperature. Note that at high temperature the curves cling to that of the 4N sample, which corresponds to the natural expectation of an identical spinon-phonon scattering strength in all samples.

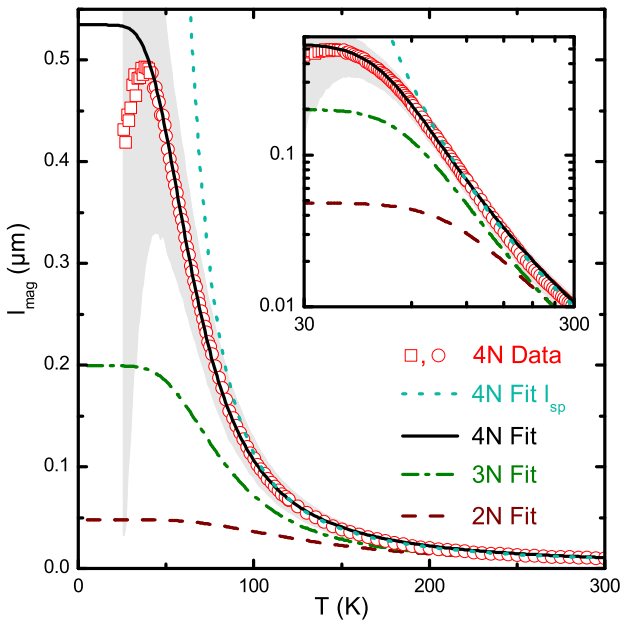

Figure 3: Derived mean free paths of the spinon excitations in Sr_2CuO_3 for 4N (circles, squares) purity. The solid black line is a fit to the data as explained in the text. The squares in the 4N data have a large uncertainty and are disregarded for the fit. A comparison is made with the fits for 2N (dashed line)[8], and 3N (dash-dotted line)[20] purities. The dotted line is a fit done to the 4N results by $l_{\rm sp}$ (eq. 2) only. The shaded area illustrates the uncertainty from the estimation of the phononic background. The inset shows the same results in a double logarithmic scale.

In order to capture this behavior in our further analysis, we apply Matthiessen's rule for the scattering processes of the spinons $l_{\rm mag}^{-1}(T) = l_0^{-1} + l_{\rm sp}^{-1}(T)$, where l_0 denotes the T-independent spinon-defect scattering, while $l_{\rm sp}(T)$ takes the T-dependent spinon-phonon scattering into account. According to our empirical finding of an exponential decay of $\kappa_{\rm mag}(T)$ at high temperature and consistent with previous findings[8,15] we estimate $l_{\rm sp}(T)$ as

$$l_{\rm sp}^{-1} = \left(\frac{\exp(T_u^*/T)}{A_s T}\right)^{-1}, \qquad (2)$$

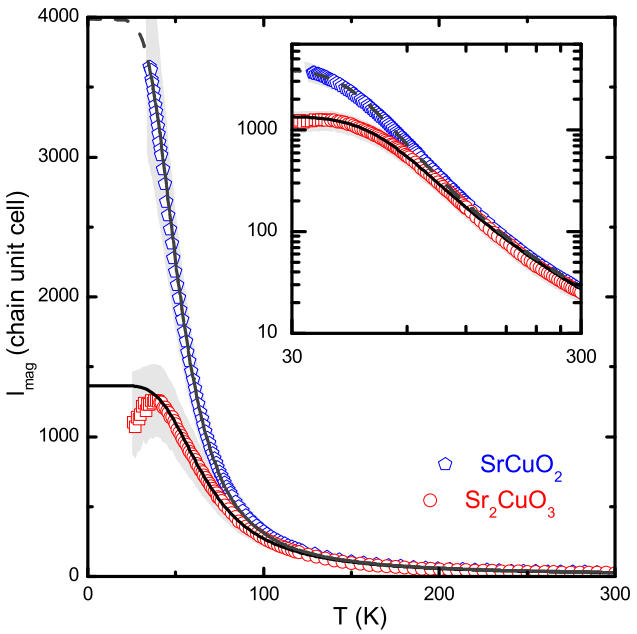

Figure 4: Magnetic mean free paths of $SrCuO_2$ (pentagon shape) and Sr_2CuO_3 (circles) for 4N purity. The shaded area illustrates the uncertainty from the estimation of the phononic background. The lines are fits to the mean free paths.

with fit parameters T_u^* and A_s. As can be seen in Fig. 3 such a empirically derived functional form for the spinon-phonon scattering allows an excellent fit of the data with $l_0 = 0.54 \pm 0.05$ µm (corresponding to approximately 1367 lattice spacings), $T_u^* = 210 \pm 11$ K, and $A_s = (6.1 \pm 5) \times 10^5 \mathrm{m}^{-1}\mathrm{K}^{-1}$.

C. Comparison of $SrCuO_2$ and Sr_2CuO_3

The drastic enhancement of κ_{mag} and l_{mag} upon increasing the purity level of Sr_2CuO_3 provides strong evidence that the spinon heat transport in the $S = 1/2$ AFM Heisenberg model as realized in this material is only limited by the *external* scattering off defects and phonons. Our findings here thus further corroborate previous experimental evidence[15] for the ballistic nature of heat transport in the $S = 1/2$ AFM Heisenberg model, obtained for the zig-zag chain compound $SrCuO_2$. Since the individual chains in $SrCuO_2$ and in Sr_2CuO_3 consists of the same structural elements (CuO_2 plaquettes), it is instructive to directly compare the findings for spinon-phonon scattering obtained for both compounds. For this purpose we show in Fig. 4 the spinon mean free path $l_{\mathrm{mag}}(T)$ of high-purity (4N) $SrCuO_2$ and Sr_2CuO_3 in units of the chain unit cells. In this representation, the mean free path is free of any geometrical particularities and can directly be related to distances of spin sites within a single chain. As can be seen in the figure, the mean free paths for both compounds are virtually identical for temperatures $T > 150$ K (the relative difference is less than 5%). In the whole temperature range, both curves can be well fitted with expression 2 for the spinon-phonon scattering, with the same T_u^*, A_s as determined afore and with and $l_0 = 1.56 \pm 0.16$ µm (corresponding to approximately 3984 lattice spacings) for $SrCuO_2$. In fact, the same parameters for $l_{\mathrm{sp}}(T)$ could be used for both compounds. This demonstrates that the spinon phonon interaction is the same in both compounds, despite the difference of their CuO_2 chain structures. Since the chains in $SrCuO_2$ and Sr_2CuO_3 are composed of the same copper-oxygen plaquettes, one has to conclude that only phonon modes which modulate the Cu-O-Cu bonds along two corner-sharing plaquettes lead to a significant scattering of spinons.

At low temperature, the mean free path of $SrCuO_2$ is by a factor of three larger than that of Sr_2CuO_3, in spite of the same nominal purity. The higher defect density of Sr_2CuO_3 may be caused by the relatively lower chemical stability. It reacts quite rapidly with water and decays, if exposed to air for a few hours. Additionally, with regard to unavoidable intrinsic crystal defects, the double chain is a much more stable structure, due to its layout of the CuO_2-plaquettes.

Apart from these minor and plausible differences with regard to the spinon heat conduction, we would like to point out a surprising dissimilarity which concerns the phonon heat conductivity κ_{ph}. As we have seen in Fig. 1, κ_{ph} of Sr_2CuO_3 increases strongly at increasing the purity, as expected. However, in $SrCuO_2$ the increase is very weak, which suggests an additional scattering mechanism for phonons in this material.[15]

D. Theoretical treatment of the spinon-phonon scattering

Expression 2 which describes the spinon-phonon scattering in our data has been empirically derived and is consistent with general considerations for Umklapp scattering. In the following we go beyond this empirical treatment and derive $l_{\mathrm{sp}}(T)$ from a spinon-phonon scattering theory presented in Ref. 46 (labelled $\tilde{l}_{\mathrm{sp}}(T)$). In this memory function approach it is possible to semi-analytically evaluate the temperature dependence of the mean-free path within the XY limit of the Heisenberg model assuming weak coupling.

Applying a Jordan-Wigner transformation the XY Hamiltonian becomes,

$$H = \sum_l h^s_{l,l+1} = -t \sum_l (1 - \lambda(x_{l+1} - x_l))(c^\dagger_{l+1} c_l + h.c.) \quad (3)$$

where $-t = J/2$ and λ is the spin-phonon coupling constant in the spin-Peierls XY model. In this tight binding model the dispersion of fermions is given by $\epsilon_k = -2t\cos(ka)$ and the velocity at the Fermi wavevector $k = \pi/2a$ is equal to $v = 2ta/\hbar$ (a is the lattice constant). In the isotropic Heisenberg model the elementary

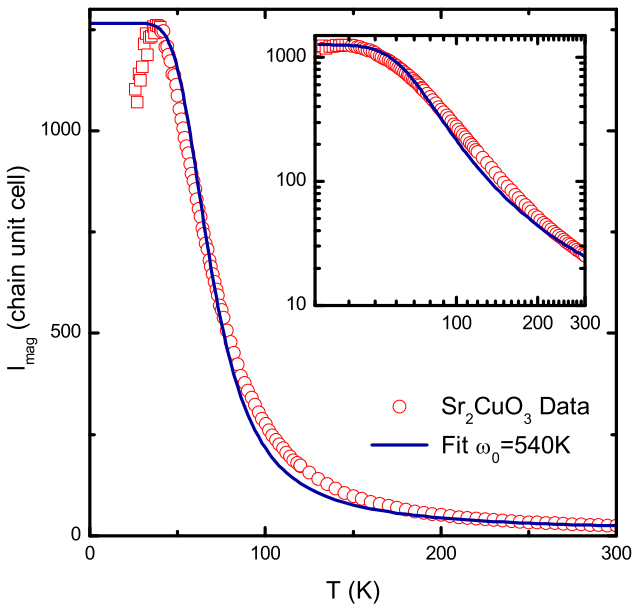

Figure 5: Fits to the mean free path according to the memory function approach explained in the text. The circles are the derived mean free paths of the spinon excitations in Sr_2CuO_3 for 4N purity. The line represent a fit using $\tilde{l}_{\rm sp}$. The parameters of the fit are $\omega_0 = 540\,\mathrm{K}$ and $l_0 = 1266$ lattice spacings ($l_0 = 4955\,\text{Å}$).

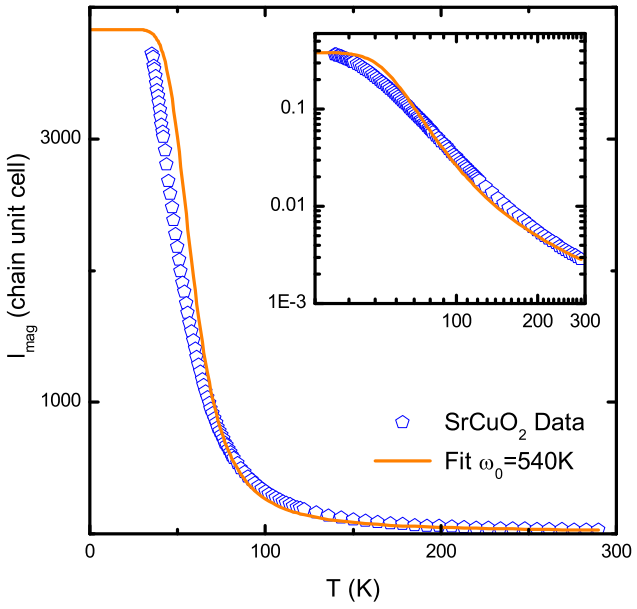

Figure 6: Fits to the mean free path according to the memory function approach explained in the text. The pentagonal shaped symbols represent the derived mean free paths of the spinon excitations in $SrCuO_2$ for 4N purity. The line represents a fit using an $l_{\rm sp}$ as defined by equation 4. The parameters of the fit are $\omega_0 = 540\,\mathrm{K}$ and $l_0 = 3831$ lattice spacings ($l_0 = 15000\,\text{Å}$).

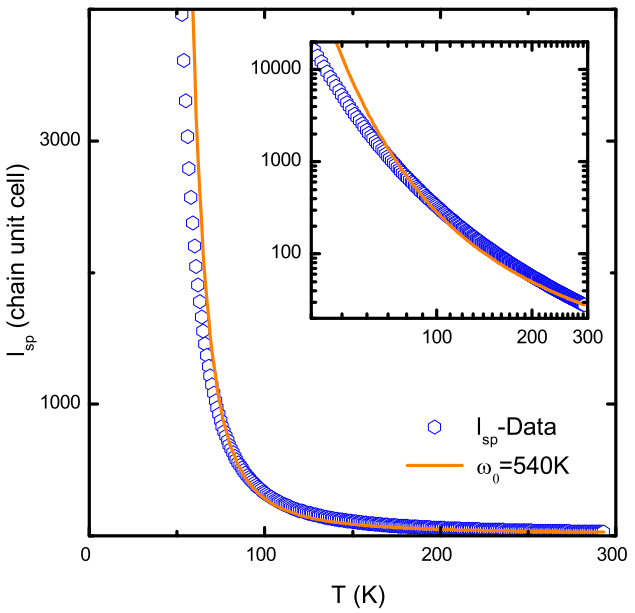

Figure 7: Comparison of the expressions for $l_{\rm sp}$ only. The hexagonal shaped symbols represent an estimate for $l_{\rm sp}$ derived from the magnetic mean free path $l_{\rm mag}$ according to $l_{\rm sp}^{-1}(T) = l_{\rm mag}^{-1}(T) - l_0^{-1}$. An $l_0 = 1.56 \pm 0.16$ µm as approximated by the phenomenological model has been used. The line represents calculations of $l_{\rm sp}$ with the memory function approach using a phonon frequency $\omega_0 = 540\,\mathrm{K}$.

magnetic excitations – the spinons – have a velocity equal to $v_{\rm sp} = \frac{\pi}{2}\frac{aJ}{\hbar}$. To take into account the difference in velocities of the excitations between the XY and isotropic Heisenberg model we evaluate the mean free path using an effective hopping matrix element $-t_{\rm eff} = \frac{\pi}{2}\frac{J}{2}$.

The mean free path is given by $\tilde{l}_{\rm sp}(T) \sim v_{\rm sp}\tau(T)$ where τ is the characteristic scattering time. The phase space of the spinon-phonon scattering matrix elements determining τ is restricted by the energy-momentum conservation laws[46] as,

$$1/\tau \sim f_k(1-f_{k+q})[(1+n_{-q})\delta(\hbar\omega+\epsilon_k-\epsilon_{k+q}-\hbar\omega_{-q}) + n_q\delta(\hbar\omega+\epsilon_k-\epsilon_{k+q}+\hbar\omega_q)]_{\omega\to 0}. \quad (4)$$

with the first term representing a phonon emission and the second, phonon absorption. $f_k = 1/(1+e^{\beta\epsilon_k})$, $n_q = 1/(e^{\beta\hbar\omega_q}-1)$ are the fermion and boson occupation factors respectively ($\beta = 1/k_BT$).

It is clear from this formulation that low energy acoustic phonons $\omega_q \sim cq$ (c the sound velocity) cannot contribute to the scattering because the energy-momentum conservation laws cannot be simultaneously satisfied. We thus consider scattering by optical phonons of frequency ω_0, as the effect of scattering by zone boundary acoustic phonons (Umklapp scattering) is similar; we take a typical $J \sim 2400\,\mathrm{K}$. In the fits shown in Fig. 5 and Fig. 6 in the temperature range $30\,\mathrm{K} < T < 300\,\mathrm{K}$ we assume $l_{\rm mag}^{-1}(T) = l_0^{-1} + \tilde{l}_{\rm sp}^{-1}(T)$ and optimize with re-

spect to l_0 (the impurity scattering length) and ω_0. As we do not know λ, we normalize the theoretical curve with respect to the experimental one at $T = 300\,\mathrm{K}$. For Sr_2CuO_3 ($SrCuO_2$) a good fit for the whole temperature range is found with $l_0 = 1266$ ($l_0 = 3831$) chain unit cells and $\omega_0 = 540\,\mathrm{K}$ for both compounds. A slightly better agreement at high temperatures can be achieved with a larger ω_0, although this leads to a strong deviation at low temperatures. The discrepancy at around 100 K is due to the fact that the model does not accurately reproduce the slope of the experimentally determined l_{sp} values below this temperature. This is illustrated in Fig. 7. There, an l_{sp} approximated from the measured data is compared to the $\tilde{l}_{\mathrm{sp}}$ as obtained from the memory function approach. The approximation of l_{sp} is done by $l_{\mathrm{sp}}^{-1}(T) = l_{\mathrm{mag}}^{-1}(T) - l_0^{-1}$, where an l_{mag} from equation 1 and the estimated $l_0 = 1.56 \pm 0.16$ µm by the phenomenological model is used. While the agreement between l_{sp} and $\tilde{l}_{\mathrm{sp}}$ is good at high temperatures, it gets poorer towards low temperatures. Especially in the double-logarithmic plot it can be seen that below 100 K the model does not reproduce the slope of the experimental estimate. It is interesting to note, that the fitted ω_0 is somewhat lower but still of the same order of magnitude than typical frequencies of the optical Cu-O stretching mode[47–50]. In contrast, the phenomenological l_{sp} according to equation 2 hints at a scattering by acoustical phonons as can be seen by the $T_u^* = 210\,\mathrm{K}$.

We mention that the exponential decay of the heat conductivity parallel to the spin chains $\kappa_b \approx \kappa_{\mathrm{mag}} \propto \exp(T_u^*/T)$ is consistent with a theoretical treatment by Shimshoni et al.[51,52]. However, we do not observe $\kappa_c = \kappa_{\mathrm{ph}} \propto \exp(2T_u^*/T)$ as is expected in the same model.

VI. SUMMARY

We have investigated the spinon thermal conductivity κ_{mag} of high-purity single crystals of the single-chain $S = 1/2$ AFM Heisenberg chain compound Sr_2CuO_3. We find that κ_{mag} is strongly enhanced as compared to previous results obtained on lower purity crystals. The analysis of the data yields a very large low-temperature mean free path of ~ 0.5µm, corresponding to 1266 chain unit cells. Upon increasing the temperature towards room temperature, the mean free path decreases strongly and approaches that observed in lower purity samples. By using a kinetic model we can decompose the mean free path into a temperature-independent spinon-defect scattering length l_0 and a temperature dependent spinon-phonon scattering length $l_{\mathrm{sp}} \sim \frac{1}{T}\exp T_u^*/T$ with a characteristic energy scale $k_B T_u^*$ for umklapp processes. and for low-T upon increasing the purity.

By comparing the temperature dependence of the mean free path of Sr_2CuO_3 with that of $SrCuO_2$, we could show that the spin-phonon interaction, as expressed by l_{sp} is practically the same in both systems. The comparison of the empirically derived l_{sp} with model calculations for the spin-phonon interaction of the $S = 1/2$ AFM XY chain model yields a reasonable agreement. This agreement is very encouraging for further studies as an analysis of the full Heisenberg model might improve this agreement even more.

	B in $10^{-31}\,\mathrm{K^{-1}s^2}$	A in $10^{-43}\,\mathrm{s^3}$	L in $10^{-4}\mathrm{m}$	b
2N	2.25	4.50	7.50	3.60
4N	3.45	1.53	2.33	3.49

Table I: Fit parameters of a Callaway fit to κ_c of Sr_2CuO_3, shown in the left panel of Fig. 1 with $\alpha = 3$ and $\beta = 1$.

Acknowledgments

We thank W. Brenig, A. L. Chernyshev, F. Heidrich-Meisner, and P. Prelovšek for fruitful discussions. Additionally, we thank W. Brenig for an important comment on the manuscript. This work was supported by the Deutsche Forschungsgemeinschaft through grant HE3439/7, through the Forschergruppe FOR912 (grant HE3439/8) and by the European Commission through the projects NOVMAG (FP6-032980) and LOTHERM (PITN-GA-2009-238475).

Appendix

In order to model the phononic thermal conductivity perpendicular to the chain, a phenomenological model, devised by Callaway[35], can be used. Although this model has undergone several revisions and extensions[53–58], the main approach is to model κ_{ph} within the Debye approximation as[59]

$$\kappa_{\mathrm{ph}} = \frac{k_B}{2\pi^2 v_{\mathrm{ph}}}\left(\frac{k_B T}{\hbar}\right)^3 \int_0^{\Theta_D/T} \frac{x^4 \mathrm{e}^x}{\left(\mathrm{e}^x - 1\right)^2} \cdot \tau_c \mathrm{d}x. \quad (5)$$

Here $x = \hbar\omega/k_B T$, ω is the phonon angular frequency, Θ_D is the Debye temperature and v_{ph} is the phonon velocity. In the Debye approximation the sound velocity is given as

$$v_s = \frac{\theta_D k_B}{\left(6\pi^2 N\right)^3 \hbar}, \quad (6)$$

with N representing the number of elementary cells per unit volume. τ_c is a combined scattering rate, which is assumed to be the sum of all individual scattering rates

$$\tau_c^{-1} = \tau_B^{-1} + \tau_D^{-1} + \tau_U^{-1}, \quad (7)$$

where τ_B denotes boundary scattering, τ_D point defect scattering and τ_U Umklapp scattering. This separation is possible, as long as these scattering processes are independent of each other, which is the gist of Matthiessen's rule. In the context of the model, this is considered to be fulfilled since in different temperature regions different

scattering mechanisms are dominant. A τ_c containing expressions for all scattering processes can then be written as

$$\tau_c^{-1} = \frac{v_{\rm ph}}{L} + A\omega^4 + B\omega^2 T \exp\left(-\frac{\Theta_D}{bT}\right), \qquad (8)$$

with fit parameters L, A, B, b. The values of these parameters are given in table I for the fit in the inset of Fig. 1. The largest changes, when comparing the two purities, are for parameter A, which describes the concentration of point defects, and for parameter L, which describes the boundary scattering. The difference in boundary scattering only indicates a difference in the sample geometries between the 2N and 4N samples. The decrease of scattering by point defects upon an increase of purity however underpins the overall reduction of defects. It should be noted that in Ref. 8 two additional scattering processes had to be used to describe the data. In our analysis which is focused on temperatures above the maximum of κ these are not necessary.

[1] S. M. Hayden, G. Aeppli, R. Osborn, A. D. Taylor, T. G. Perring, S.-W. Cheong, and Z. Fisk, Phys. Rev. Lett. **67**, 3622 (1991).
[2] T. Thio, T. R. Thurston, N. W. Preyer, P. J. Picone, M. A. Kastner, H. P. Jenssen, D. R. Gabbe, C. Y. Chen, R. J. Birgeneau, and A. Aharony, Phys. Rev. B **38**, 905 (1988).
[3] E. Dagotto and T. M. Rice, Science **271**, 618 (1996).
[4] E. Dagotto, Rep. Prog. Phys. **62**, 1525 (1999).
[5] N. Motoyama, H. Eisaki, and S. Uchida, Phys. Rev. Lett. **76**, 3212 (1996).
[6] A. V. Sologubenko, K. Giannò, H. R. Ott, U. Ammerahl, and A. Revcolevschi, Phys. Rev. Lett. **84**, 2714 (2000).
[7] A. V. Sologubenko, E. Felder, K. Giannò, H. R. Ott, A. Vietkine, and A. Revcolevschi, Phys. Rev. B **62**, R6108 (2000).
[8] A. V. Sologubenko, K. Giannò, H. R. Ott, A. Vietkine, and A. Revcolevschi, Phys. Rev. B **64**, 054412 (2001).
[9] C. Hess, C. Baumann, U. Ammerahl, B. Büchner, F. Heidrich-Meisner, W. Brenig, and A. Revcolevschi, Phys. Rev. B **64**, 184305 (2001).
[10] C. Hess, H. ElHaes, B. Büchner, U. Ammerahl, M. Hücker, and A. Revcolevschi, Phys. Rev. Lett. **93**, 027005 (2004).
[11] C. Hess, C. Baumann, and B. Büchner, J. Mag. Mag. Mater. **290-291**, 322 (2005).
[12] C. Hess, P. Ribeiro, B. Büchner, H. ElHaes, G. Roth, U. Ammerahl, and A. Revcolevschi, Phys. Rev. B **73**, 104407 (2006).
[13] C. Hess, B. Büchner, U. Ammerahl, L. Colonescu, F. Heidrich-Meisner, W. Brenig, and A. Revcolevschi, Phys. Rev. Lett. **90**, 197002 (2003).
[14] C. Hess, H. ElHaes, A. Waske, B. Büchner, C. Sekar, G. Krabbes, F. Heidrich-Meisner, and W. Brenig, Phys. Rev. Lett. **98**, 027201 (2007).
[15] N. Hlubek, P. Ribeiro, R. Saint-Martin, A. Revcolevschi, G. Roth, G. Behr, B. Büchner, and C. Hess, Phys. Rev. B **81**, 020405(R) (2010).
[16] N. Hlubek, P. Ribeiro, R. Saint-Martin, S. Nishimoto, A. Revcolevschi, S.-L. Drechsler, G. Behr, J. Trinckauf, J. E. Hamann-Borrero, J. Geck, et al., Phys. Rev. B **84**, 214419 (2011).
[17] X. Zotos, F. Naef, and P. Prelovsek, Phys. Rev. B **55**, 11029 (1997).
[18] X. Zotos, Phys. Rev. Lett. **82**, 1764 (1999).
[19] T. Kawamata, N. Kaneko, M. Uesaka, M. Sato, and Y. Koike, Journal of Physics: Conference Series **200**, 022023 (2010).
[20] T. Kawamata, N. Takahashi, T. Adachi, T. Noji, K. Kudo, N. Kobayashi, and Y. Koike, J. Phys. Soc. Jpn. **77**, 034607 (2008).
[21] C. L. Teske and H. Müller-Buschbaum, Z. Anorg. Allg. Chem. **371**, 325 (1969).
[22] T. Ami, M. K. Crawford, R. L. Harlow, Z. R. Wang, D. C. Johnston, Q. Huang, and R. W. Erwin, Phys. Rev. B **51**, 5994 (1995).
[23] H. Suzuura, H. Yasuhara, A. Furusaki, N. Nagaosa, and Y. Tokura, Phys. Rev. Lett. **76**, 2579 (1996).
[24] A. Keren, L. P. Le, G. M. Luke, B. J. Sternlieb, W. D. Wu, Y. J. Uemura, S. Tajima, and S. Uchida, Phys. Rev. B **48**, 12926 (1993).
[25] K. M. Kojima, Y. Fudamoto, M. Larkin, G. M. Luke, J. Merrin, B. Nachumi, Y. J. Uemura, N. Motoyama, H. Eisaki, S. Uchida, et al., Phys. Rev. Lett. **78**, 1787 (1997).
[26] I. A. Zaliznyak, H. Woo, T. G. Perring, C. L. Broholm, C. D. Frost, and H. Takagi, Phys. Rev. Lett. **93**, 087202 (2004).
[27] T. M. Rice, S. Gopalan, and M. Sigrist, Europhys. Lett. **23**, 445 (1993).
[28] M. Matsuda, K. Katsumata, K. M. Kojima, M. Larkin, G. M. Luke, J. Merrin, B. Nachumi, Y. J. Uemura, H. Eisaki, N. Motoyama, et al., Phys. Rev. B **55**, R11953 (1997).
[29] I. A. Zaliznyak, C. Broholm, M. Kibune, M. Nohara, and H. Takagi, Phys. Rev. Lett. **83**, 5370 (1999).
[30] A. Revcolevschi, U. Ammerahl, and G. Dhalenne, J. Cryst. Growth **198**, 593 (1999).
[31] R. Scholder, R. Felsenstein, and A. Apel, Z. anorg. allg. Chem. **216**, 138 (1933), ISSN 1521-3749.
[32] J. M. Hill, D. C. Johnston, and L. L. Miller, Phys. Rev. B **65**, 134428 (2002).
[33] C. Hess, B. Büchner, U. Ammerahl, and A. Revcolevschi, Phys. Rev. B **68**, 184517 (2003).
[34] R. Berman, *Thermal Conduction in Solids* (At the Clarendon Press, Oxford, 1976).
[35] J. Callaway, Phys. Rev. **113**, 1046 (1959).
[36] A. V. Rozhkov and A. L. Chernyshev, Phys. Rev. Lett. **94**, 087201 (2005).
[37] A. L. Chernyshev and A. V. Rozhkov, Phys. Rev. B **72**, 104423 (2005).
[38] A. Klümper and K. Sakai, J. Phys. A: Math. Gen. **35**, 2173 (2002).
[39] F. Heidrich-Meisner, A. Honecker, D. C. Cabra, and W. Brenig, Phys. Rev. B **66**, R140406 (2002).
[40] F. Heidrich-Meisner, A. Honecker, D. C. Cabra, and W. Brenig, Phys. Rev. B **68**, 134436 (2003).
[41] F. Heidrich-Meisner, A. Honecker, and W. Brenig, Phys.

Rev. B **71**, 184415 (2005).
[42] A. Chernyshev, J. Magn. Magn. Mater. **310**, 1263 (2007), ISSN 0304-8853.
[43] S. Gangadharaiah, A. L. Chernyshev, and W. Brenig, Phys. Rev. B **82**, 134421 (2010).
[44] N. W. Ashcroft and N. D. Mermin, *Solid State Physics* (Brooks Cole, 1976).
[45] C. Hess, Eur. Phys. J. Special Topics **151**, 73 (2007).
[46] K. Louis, P. Prelovšek, and X. Zotos, Phys. Rev. B **74**, 235118 (2006).
[47] Y. S. Lee, T. W. Noh, H. S. Choi, E. J. Choi, H. Eisaki, and S. Uchida, Phys. Rev. B **62**, 5285 (2000).
[48] Z. Popovic, M. Konstantinovic, R. Gajic, C. Thomsen, U. Kuhlmann, and A. Vietkin, Physica C **351**, 386 (2001).
[49] M. Grüninger, D. van der Marel, A. Damascelli, A. Erb, T. Nunner, and T. Kopp, Phys. Rev. B **62**, 12422 (2000).
[50] M. Windt, M. Grüninger, T. Nunner, C. Knetter, K. P. Schmidt, G. S. Uhrig, T. Kopp, A. Freimuth, U. Ammerahl, B. Büchner, et al., Phys. Rev. Lett. **87**, 127002 (2001).
[51] E. Shimshoni, N. Andrei, and A. Rosch, Phys. Rev. B **68**, 104401 (2003).
[52] E. Shimshoni, N. Andrei, and A. Rosch, Phys. Rev. B **72**, 059903 (2005).
[53] J. Callaway and H. C. von Baeyer, Phys. Rev. **120**, 1149 (1960).
[54] J. Callaway, Phys. Rev. **122**, 787 (1961).
[55] S. Simons, Phys. Status Solidi B **53**, K41 (1972).
[56] J. Callaway, *Quantum Theory of the Solid State* (Academic Press, 1991).
[57] K. C. Sood and M. K. Roy, J. Phys.: Condens. Matter **5**, L245 (1993).
[58] J. D. Chung, A. J. H. McGaughey, and M. Kaviany, Journal of Heat Transfer **126**, 376 (2004).
[59] R. Berman, *Thermal conduction in solids* (Clarendon Press, Oxford, 1976).